

# A 4D EMITTANCE MEASUREMENT DEVICE FOR THE 870 keV HIPA INJECTION LINE

R. Dölling<sup>†</sup>, M. Rohrer, Paul Scherrer Institut, 5232 Villigen PSI, Switzerland

## Abstract

A 4D emittance measurement device has recently been installed in PSI's high intensity proton accelerator (HIPA) after the acceleration tube of the Cockcroft-Walton pre-accelerator. A pinhole collimator is moved 2D transversally and at each collimator position, the resulting beamlet is downstream scanned 2D by vertically moving over it a horizontal linear array of small electrodes. The properties of this setup and the intended use are discussed.

## INTRODUCTION

In HIPA [1-3] a 10 mA DC proton beam is extracted [4] from a microwave driven volume source [5]. It is matched by a nearly fully space-charge compensated two-solenoid LEBT [4] to a 810 keV electrostatic acceleration tube driven by a Cockcroft-Walton [6]. In a 870 keV transport line of magnetic quadrupoles [3, 7] the beam is bunched [8, 3] and matched to the Injector 2 cyclotron [9], where it is collimated at the first five turns to the production current of 2.2 mA [10, 11, 3]. The space charge dominated bunches are rolled up [12-17] during acceleration and the CW 50 MHz bunched beam of 72 MeV and 2.2 mA is matched by another transport line of magnetic quadrupoles to the Ring cyclotron, where the beam is accelerated to 590 MeV [18, 3, 19]. After extraction [20], it is sent via the targets M and E, producing muons and pions, to the spallation neutron source SINQ [21, 22], or alternatively switched to the ultra-cold neutron source UCN for a few seconds every few minutes [23].

Limitation of beam losses above a few MeV and of the resulting activation of machine components is important. Guided by Joho's  $N^{-3}$  scaling law [24-26] the RF cavities in the Ring cyclotron were replaced, almost doubling their accelerating voltages [1, 25], and the beam current could be raised over the years at a constant level of beam losses. The sensitivity of the losses in the Ring cyclotron to the settings of ion source and collimation at the first turns of Injector 2 [3] as well as the positive effect of scraping the beam at certain collimators in the 870 keV injection line [27] indicate that a further reduction of beam losses at higher energies can be expected for a refined collimation in the 870 keV line and the centre region of Injector 2.

In a production machine such substantial hardware changes must be well-directed. A detailed understanding of the transport of beam core and halo based on "advanced beam dynamics simulations" including detailed 6D beam distributions and space charge is required [28, 29]. Simulations of this type were performed for segments of the accelerator chain [14, 18, 30-33], but only idealized starting distributions were used. A start-to-end simulation and a more detailed machine model are still under development.

The need for these simulations was also demonstrated by the failed commissioning of the superbuncher [29, 30, 34] which caused too large beam losses. (In contrary to the bunchers in the 870 keV line, badly affected beam particles cannot be collimated downstream at low activation cost.) Further analytical studies, such as [35], are needed to support the development of simulation tools.

Simulations as presented in [36] would also allow to determine the degree and effect of space-charge compensation (SCC) in the 870 keV transport line from a comparison with measured beam profiles. However, the use of oversimplified simulations of only a part of the line [37] is not conclusive. A measurement of the local compensation in a drift section of the line [38] indicated a compensation degree of 44% at  $1e-4$  mbar, and only 11% at  $1.2e-5$  mbar,  $N_2$  gas pressure, which is still about a factor of 3 above the  $N_2$  gas pressure at standard operation. This result cannot, however, simply be extrapolated into the magnets and to the full line since the distribution of the compensation electrons is affected by the magnetic fields, the bunching and other parameters [36, 39].

Most changes in collimation and beam optics were realized in the early years of operation. This was guided by beam dynamics considerations, educated guesses, simulations using Transport, Turtle [40] and other codes. Extensive empirical tuning by the operators played a significant part in the optimization. However, there is still potential for optimisations which do not require hardware changes; e.g. the tests of a "smooth" beam optic in the 870 keV beam line [41], which should result in a lower emittance growth, could be pursued. Only minor optics modifications have been implemented since 2006, such as an even lower numbers of turns in the cyclotrons and a dispersion free section in the 72 MeV beam line [29]. In spite of having not contributed to the optics of the production beam up to now, "advanced" simulations are the most promising approach to significant improvements.

The 4D emittance measurement (<sup>4D</sup>EM) should provide simulations of downstream and upstream beam transport with a detailed truly 4D start distribution of the 870 keV 10 mA  $H^+$  beam leaving the acceleration tube (Fig. 1). However, we also expect evidence on the reproducibility of ion source and SCC in the 60 keV LEBT. Similar to the bunch-shape measurements at higher energies [42], the <sup>4D</sup>EM is not intended as a tool for daily operation, but for beam dynamics development purposes.

## SETUP

The <sup>4D</sup>EM has been squeezed into the beginning of the 870 keV transport line, without changing the quadrupole positions (Figs. 1 and 2) by removing an unused slit and integrating existing collimators for machine protection into its two vacuum chambers.

<sup>†</sup> rudolf.doelling@psi.ch

Content from this work may be used under the terms of the CC BY 3.0 licence (© 2018). Any distribution of this work must maintain attribution to the author(s), title of the work, publisher, and DOI.

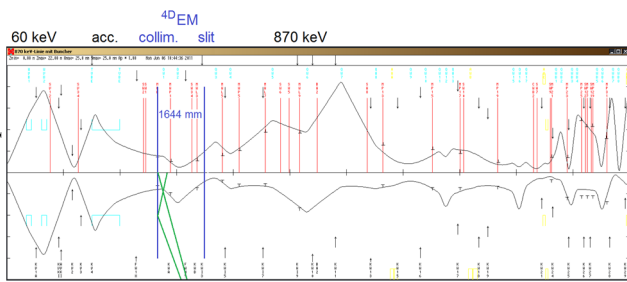


Figure 1: Beam transport from ion source to Injector 2 cyclotron. Vertical (above) and horizontal (below)  $2\sigma$  envelopes from Transport [40] fit to measured profile width. SCC is included only as correction factors to space charge. Green lines indicate the beam divergence which is accepted by the  $4^{\text{D}}\text{EM}$  at axis and 10 mm away from it.

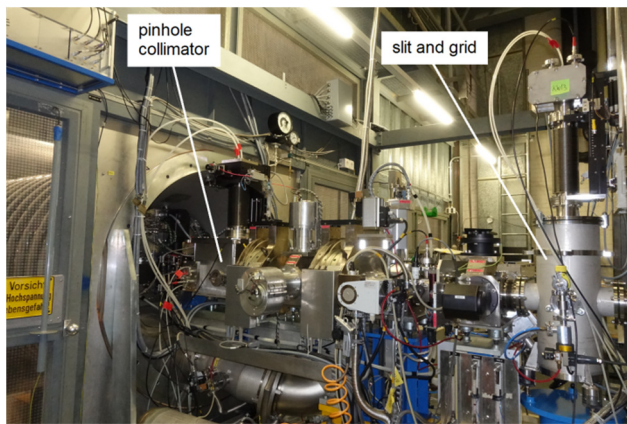


Figure 2:  $4^{\text{D}}\text{EM}$  in 870-keV beam line.

### Pinhole Collimator

The upstream vacuum chamber houses a cooled collimator which, if inserted, stops the full beam with the exception of a 0.3 mm diameter beamlet (Fig. 3). The collimator can be moved vertically and horizontally for  $\pm 20$  mm by a 2-axis feedthrough driven by stepper motors. This allows to scan the slightly convergent circular beam of  $\sim 10$  mm core diameter.

A fixed pre-collimator of 40 mm x 40 mm aperture cuts the beam tails. In between, a suppressor electrode biased to  $-600$  V prevents secondary electrons from the collimator to change SCC in the preceding 1.2 m drift space. The bias is maintained when the  $4^{\text{D}}\text{EM}$  is not used.

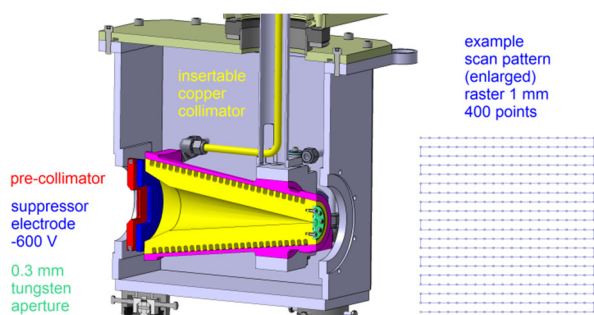


Figure 3: Upstream chamber with pinhole collimator.

Cooling grooves are milled into the collimators OFHC copper body and covered by a brazed 1.4435 stainless steel jacket. The pinhole aperture is eroded into a tungsten insert screwed to the copper block. If the device is not used, the water speed is reduced from 5 to 1 m/s to prevent corrosion.

### Thermal Load

Thermal demands to the collimator are high, especially with the beam off-centre. (A pepperpot was not considered for this reason.) Due to the short length and the large transverse measurement range, it cannot handle the full beam power. The critical parameter in the chosen design is the yield stress. The yield stress index (YSI), the ratio of von-Mises stress to yield stress, should stay below 1.0 to prevent thermomechanical failure of the copper [43]. Simulations were performed with Comsol [44] assuming a Gaussian beam with  $\sigma_x = \sigma_y = 2.5$  mm which couples into the cone surface, the temperature dependent copper yield stress used in [43] and a thermal resistance of 28 K/(W/mm<sup>2</sup>) of the copper-water boundary at the cooling channel surface. Accordingly a reduction of beam power to 2.5 kW is needed to satisfy the YSI criterion. At the same time copper temperatures and power densities at the cooling channel are moderate (Fig. 4).

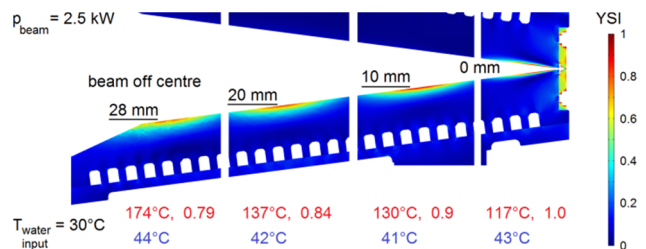


Figure 4: YSI for four different beam offsets. The plot is combined from four simulations, showing only the regions with large YSI values. Red: Maxima of copper temperature and YSI. Blue: Maxima of copper temperature at water boundary.

This will constrain operation to pulsed beam with a duty cycle of up to 25 %. Pulsing with an adjustable duty cycle is provided by deflecting the beam at the end of the LEBT with a fast kicker magnet at a rate of 500 Hz. The effect of pulsing to the SCC along the drift space from acceleration tube to collimator has to be determined.

### Slit and Grid

In the downstream chamber, a slit is scanned vertically over the beamlet for up to 80 mm (Fig. 5). Behind the slit a co-moving grid of readout electrodes is formed by a stack of 160 0.4 mm thick copper sheets, isolated by 100  $\mu\text{m}$  Kapton foils. The foils are retracted at the face and the stack is tilted by  $4^\circ$  in order to hide the foils from the beam. The slit base plate is water cooled. During measurement, the water speed is reduced from 7 to 1.3 m/s to decrease microphonic noise.

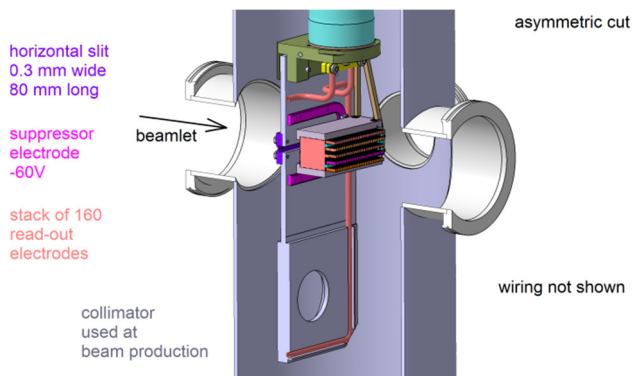


Figure 5: Downstream chamber with slit and grid.

## Electronics

The three stepper motors are controlled by a 4-channel Meson-VME module [45], which also measures the signal currents at pre-collimator, collimator and slit plate. This module also sends a trigger impulse to the five 32-channel LogIV [46], which then read the 160 grid signals as a waveform in coincidence with the trajectory of the slit.

## MEASUREMENT PROCEDURE

### Envisaged Measurement Procedure

Before inserting collimator and slit, the beam is switched off and the in-between quadrupoles QWA1/2 are de-gaussed. With water flows adjusted and collimator and slit moved to start positions, the beam is switched on and the measurement sequence begins: The slit moves downward by, e.g., 80 mm at a constant speed of 25 mm/s and the grid currents are measured in parallel at a rate of 50 samples/s, each averaged over 20 ms. (Short ramps are added for acceleration and deceleration.) Then the collimator moves to the next point, followed by an upward scan of the slit. The collimator trajectory, e.g., as in Fig. 3, will be executed within ~26 minutes.

### Estimated Performance

This demonstrates that the resolution (in this case, 1 mm spatial and 0.31 mrad angular) is in practice restricted by available measurement time and beam stability. Accuracy and reproducibility will also depend on the quality of de-gaussing of the in-between quadrupoles.

The full angular range allows to display fractions of  $H_2^+$  and  $H_3^+$  (within the spatial range), which survived magnetic filtering in the LEBT and are separated by a steerer magnet located 0.52 m upstream of the collimator aperture. Measurement time may be halved by reducing the  $\pm 24$  mrad angular range vertically to the perimeter of the  $H^+$  emittance distribution.

At a 10 mA pulsed beam at 10% duty cycle, the largest signal current (averaged over the pulsing) at a single grid electrode is estimated to 10 nA. With a lower current limit of the LogIV of a few pA, a dynamic range of phase space density of 1000 results. Other than in a pepperpot measurement, no information is lost by an overlap of angular distributions of beamlets.

## PROTECTION

End switches control the position of the drives to prevent thermal overload. The beam is switched off if the pinhole collimator is in transit from its parking to working position or if the slit is moved in when the collimator is not at the working position. Furthermore, all water circuits are supervised for sufficient flow and upper limits for the signal currents from collimators and slit are enforced.

It is difficult to safely protect the pinhole collimator against overly focused beam which may lead to severe damage. Limits will be set to the solenoid currents in the LEBT to keep beam size within a certain range. Beam size can also be checked with the upstream beam-induced fluorescence monitor [47]. However, supervision will still be less stringent and redundant than e.g. at the 72-MeV beam dump BX2 after the Injector 2 [48].

## OUTLOOK

The project is presently on hold due to a lack of resources. The measurement software has still to be written, including suitable depictions of the 4D distribution which is not directly displayed as in the case of the pepperpot with screen. In addition to commissioning we will attempt to improve the thermal capability towards full current operation. We will also seek a better understanding of the fatigue limit of the present collimator configuration.

## ACKNOWLEDGEMENTS

We thank Mischa Tahedl for creating the 3D model and the drawings and contributing to supervision of manufacturing and acquisition of components, Roger Senn for mounting, testing and inserting the mechanics, Urban Frei and Gregor Gamma for installing the electronics and testing, and Hubert Lutz and Patric Bucher for integration into the machine control system and run permit system.

## AUTHOR CONTRIBUTIONS

RD conceived the device, specified its physics layout and wrote the paper. MR provided the detailed mechanical layout and contributed to the figures.

## REFERENCES

- [1] M. Seidel *et al.*, “Production of a 1.3 MW proton beam at PSI”, in *Proc. IPAC'10*, Kyoto, Japan, May 2010, paper TUYRA03, pp. 1309-1313.
- [2] M. Seidel *et al.*, “High intensity operation and control of beam losses in a cyclotron based accelerator”, in *Proc. HB'12*, Beijing, China, Sept. 2012, paper THO1C01, pp. 555-559.
- [3] T. Stambach *et al.*, “The PSI 2 mA beam and future applications”, in *Proc. Cyclotrons'01*, East Lansing, MI, USA, May 2001, pp. 423-427.
- [4] M. Olivo, “Operational experience with the SIN 870 keV Cockcroft-Walton pre-injector”, in *Proc. Cyclotrons'86*, Tokyo, Japan, Oct. 1986, pp. 519-522.
- [5] C. Baumgarten *et al.*, “A compact electron cyclotron resonance proton source for the Paul Scherrer Institute’s proton

- accelerator facility”, *Rev. Sci. Instrum.*, vol. 82, p. 053304, May 2011, doi :10.1063/1.3590777
- [6] M. Olivo, “Initial operation of the SIN 860 keV Cockcroft-Walton pre-injector”, in *Proc. Linac’84*, Seeheim, Germany, May 1984, pp. 380-382.
- [7] C. Markovits *et al.*, “The 870 keV high intensity proton beam transfer line for the Injector 2 cyclotron at SIN”, in *Proc. PAC’87*, Washington, D:C., USA, Mar. 1987, pp. 1954-1956.
- [8] G. Grillenberger *et al.*, “Commissioning and tuning of the new buncher system in the 870 keV injection beamline”, in *Proc. Cyclotrons’07*, Giardini Naxos, Italy, Oct. 2007, pp. 464-466.
- [9] W. Joho *et al.*, “Commissioning of the new high intensity 72 MeV Injector II for the SIN Ring cyclotron”, in *Proc. PAC’85*, Vancouver, BC, Canada, May 1985, pp. 2666-2668.
- [10] J. Stetson *et al.*, “The commissioning of PSI Injector 2 for high intensity, high quality beams”, in *Proc. Cyclotrons’92*, Vancouver, BC, Canada, July 1992, pp. 36-39.
- [11] A. Kolano, “A precise 3D beam dynamics model of the PSI Injector II”, Ph.D. thesis, University of Huddersfield, Huddersfield, UK, 2017, <http://eprints.hud.ac.uk/id/eprint/31753/>
- [12] S. Adam, “Calculation of space-charge effects in isochronous cyclotrons”, in *Proc. PAC’85*, Vancouver, BC, Canada, May 1985, pp. 2507-2509.
- [13] S. R. Koscielniak *et al.*, “Simulation of space-charge dominated beam dynamics in an isochronous AVF cyclotron”, in *Proc. PAC1993*, Washington, D.C., USA, May 1993, pp. 3639-3641.
- [14] J. J. Yang *et al.*, “Beam dynamics in high intensity cyclotrons including neighboring bunch effects: Model, implementation, and application”, *Phys. Rev. ST Accel. Beams*, vol. 13, p. 064201, Jun. 2010, doi :10.1103/PhysRevSTAB.13.064201
- [15] A. Goto, “Mechanism of formation of a round beam by space-charge forces in cyclotrons”, *RIKEN Accel. Prog. Rep.* Vol 44, 2011, pp. 107-108.
- [16] R. Baartman, “Space charge limit in separated turn cyclotrons”, in *Proc. Cyclotrons’13*, Vancouver, BC, Canada, Sep. 2013, paper WE2PB01, pp. 305-309.
- [17] C. Baumgarten, “Transverse-longitudinal coupling by space charge in cyclotrons”, in *Proc. Cyclotrons’13*, Vancouver, BC, Canada, Sep. 2013, paper WE2PB03, pp. 315-319.
- [18] Y. J. Bi *et al.*, “Towards quantitative simulations of high power proton cyclotrons”, *Phys. Rev. ST Accel. Beams*, vol. 14, p. 054402, May 2011, doi :10.1103/PhysRevSTAB.14.054402
- [19] W. Joho, “High intensity beam acceleration with the SIN cyclotron facility”, in *Proc. Cyclotrons’86*, Tokyo, Japan, Oct. 1986, pp. 31-37.
- [20] M. Olivo, “The electrostatic extractor channel for the SIN 590 MeV Ring cyclotron”, in *Proc. Cyclotrons’75*, Zurich, Switzerland, Aug. 1975, pp. 292-296.
- [21] U. Rohrer, “590 MeV proton beam lines”, [aea.web.psi.ch/Urs\\_Rohrer/MyWeb/pkana1.htm](http://aea.web.psi.ch/Urs_Rohrer/MyWeb/pkana1.htm)
- [22] D. Reggiani, “Extraction, transport and collimation of the PSI 1.3 MW proton beam”, in *Proc. HB’12*, Beijing, China, Sep. 2012, paper WEO3A03, pp. 373-377.
- [23] D. Reggiani *et al.*, “A macro-pulsed 1.2 MW proton beam for the PSI ultra cold neutron source”, in *Proc. PAC’09*, Vancouver, BC, Canada, May 2009, paper TU6RFP086, pp. 1748-1750.
- [24] W. Joho, “High intensity problems in cyclotrons”, in *Proc. Cyclotrons’81*, Caen, France, Sept. 1981, pp. 337-347.
- [25] T. Stambach *et al.*, “Potential of cyclotron based accelerators for energy production and transmutation”, in *Int. Conf. on Accelerator-Driven Transmutation Technologies and Applications*, Las Vegas, NM, USA, July 1994, AIP Conf. Proc. 346, 1995, pp. 229-235, doi :10.1063/1.49093
- [26] U. Schryber *et al.*, “High power operation of the PSI accelerators”, in *Proc. Cyclotrons’95*, Cape Town, South Africa, Oct. 1995, pp. 32-38.
- [27] G. Fabian, PSI, private communication, 2001.
- [28] A. Adelmann *et al.*, “Precise simulations of high-intensity cyclotrons”, PSI Scientific Report 2010, Villigen, Switzerland, pp. 54-55.
- [29] M. Humbel *et al.*, “Tuning of the PSI 590 MeV Ring cyclotron for accepting and accelerating a rebunched 72 MeV proton beam”, in *Proc. Cyclotrons’13*, Vancouver, BC, Canada, Sep. 2013, paper TH1PB02, pp. 437-439.
- [30] A. Adelmann *et al.*, “Beam dynamics studies of the 72 MeV beamline with a super buncher”, in *Proc. EPAC’04*, Lucerne, Switzerland, July 2004, paper WEPLT048, pp. 1945-1947.
- [31] A. Adelmann *et al.*, “Recent results on simulations of high intensity beams in cyclotrons”, in *Proc. Cyclotrons’04*, Tokyo, Japan, Oct. 2004, pp. 425-429.
- [32] S. Wei *et al.*, “Update on the IW2 transfer line simulations”, presented at PSI, Villigen, Switzerland, March 6, 2012, unpublished.
- [33] N. J. Pogue *et al.*, “OPAL simulations of the PSI Ring cyclotron and a design for a higher order mode flat top cavity”, in *Proc. IPAC’17*, Copenhagen, Denmark, May 2017, pp. 3891-3894, doi :10.18429/JACoW-IPAC2017-THPAB077.
- [34] M. Humbel *et al.*, “Experience with and theoretical limits of high intensity high brightness hadron beams accelerated by cyclotrons”, in *Proc. HB’04*, Bensheim, Germany, Oct. 2004, *AIP Conf. Proc.* 773, 2005, pp. 313-317, doi :10.1063/1.1949553
- [35] C. Baumgarten, “Cyclotron closed orbits on a radial grid”, *Nucl. Instr. Meth. A*, vol. 647, pp. 31-33, 2014, doi :10.1016/j.nima.2014.11.022
- [36] D. Noll *et al.*, “The particle-in-cell code bender and its application to non-relativistic beam transport”, in *Proc. HB2014*, East Lansing, MI, USA, Oct. 2014, paper WEO4LR02, pp. 304-308.
- [37] S. Adam *et al.*, “Steps to enhance the knowledge on space charge effects”, in *Proc. Cyclotrons’01*, East Lansing, MI, USA, May 2001, pp. 428-430.
- [38] J. Sherman *et al.*, “H<sup>+</sup> beam neutralization measurements at 870 keV beam energy”, *Rev. Sci. Instrum.*, vol. 63, pp. 2776-2778, Apr. 1992.
- [39] R. Dölling *et al.*, “Radial distribution of space-charge force in compensated positive-ion beams”, in *Proc. ICIS’97*, Taormina, Italy, Sep. 1997, *Rev. Sci. Instrum.*, vol. 69, pp. 1094-1099, doi :10.1063/1.1148650

- [40] U. Rohrer, PSI Graphic Transport Framework based on a CERN-SLAC-FERMILAB version by K. L. Brown *et al.*, [http://aea.web.psi.ch/Urs\\_Rohrer/MyWeb](http://aea.web.psi.ch/Urs_Rohrer/MyWeb)
- [41] R. Dölling, “Sanfte Optik in der 870-keV-Linie”, PSI, Villigen, Switzerland, Internal Rep. HIPA-BEAMDY-DR84-008.00-080310, Mar. 2010.
- [42] R. Dölling, “Progress with bunch-shape measurements at PSI’s high-power cyclotrons and beam lines”, in *Proc. HB’12*, Beijing, China, Sep. 2012, paper MOP253, pp. 187-191.
- [43] Y. Lee *et al.*, “Simulation based optimization of a collimator system at the PSI proton accelerator facilities”, in *Proc. IPAC’10*, Kyoto, Japan, May 2010, paper THPEC088, pp. 4260-4262.
- [44] COMSOL Multiphysics, release 5.3a, <http://www.comsol.com>
- [45] E. Johansen, “VME Meson design specification”, PSI, Villigen, Switzerland, Jun. 2010, unpublished.
- [46] P. A. Duperrex *et al.*, “Latest diagnostic electronics development for the Proscan proton accelerator”, in *Proc. BIW’04*, Knoxville, TN, USA, May 2004, *AIP Conf. Proc.*, vol. 732, pp. 268-275, 2004.
- [47] L. Rezzonico *et al.*, “A profile monitor using residual gas”, in *Proc. Cyclotrons’89*, Berlin, Germany, May 1989, pp. 313-316.
- [48] L. Rezzonico *et al.*, “Surveillance protection of a 150 kW proton beam dump”, in *Proc. BIW’00*, Cambridge, MA, USA, May 2000, *AIP Conf. Proc.*, vol. 546, pp. 555-562, 2000.